

## Tailoring magnetic properties of metallic thin films with quantum well states and external electric fields

T. R. Dasa, P. Ruiz-Díaz, O. O. Brovko, and V. S. Stepanyuk

*Max-Planck-Institut für Mikrostrukturphysik Weinberg 2, D-06120 Halle, Germany*

(Received 6 June 2013; published 12 September 2013)

Thickness dependence of magnetic anisotropy energy (MAE) and spin polarization in Fe and Co multilayers on a Pt(001) substrate are investigated with *ab initio* techniques. As the thickness of the thin films is increased, an oscillatory behavior of the MAE of the systems is observed. For Fe multilayers, this even results in the periodic switching of the easy axis from out of plane to in plane. Capping the multilayers with Pt, in most cases, leads to a strong enhancement of the MAE. Our calculations give clear evidence that such oscillatory behavior of MAE can be attributed to spin-polarized quantum well states (QWS) existing in thicker multilayers. The spin polarization of the QWS is also shown to have a profound thickness dependence. Finally, we show that both MAE and spin polarization of the QWS are sensitive to external electric field and can be tailored therewith.

DOI: [10.1103/PhysRevB.88.104409](https://doi.org/10.1103/PhysRevB.88.104409)

PACS number(s): 71.15.Mb, 73.22.-f, 75.30.Gw, 75.70.-i

### I. INTRODUCTION

Modern engineering applications in nanotechnology often involve the use of thin films. When such components of electronic devices are scaled down to nanometers, quantum size effect becomes important, and many electronic properties of the nanostructures can be directly related to its presence.<sup>1,2</sup> Besides, confinement of electrons at this scale leads to the formation of discrete energy levels, i.e., quantum well states (QWS).<sup>3</sup> One-dimensional (1D) QWS in thin adsorbate films can affect the electronic structure and spin polarization of the surface,<sup>4-7</sup> and thus the MAE of the system.<sup>8</sup> Basically, the physics of QWS is well understood: QWS exist as a result of delocalized electrons, being confined in a potential well.<sup>9</sup> In thin adsorbate films, the bounding potentials of the substrate and vacuum determine the confinement state that affects the properties mentioned above. If the potential or the band structure of the delocalized electrons is spin polarized, then the QWS will manifest spin-dependent character.<sup>10,11</sup> In prototype metal films, e.g., Ag/Fe(001), the existence of spin-polarized QWS with *s, p* character originated from the spin-dependent boundary conditions of the magnetic substrate were demonstrated.<sup>1</sup>

Further investigations on low-dimensional magnetic systems, which are the major candidates for spintronics technology, have shown noticeable quantum confinement features.<sup>10,12,13</sup> For instance, an oscillatory magnetic anisotropy dependence was measured as result of the variation of the thickness of the Cu overlayer deposited on a Co thin film.<sup>14</sup> This suggests that the *s, p* QWS modulate the magnetic properties of Cu/Co(001) interface.<sup>14,15</sup> Spin-polarized QWS could also be used for the transmission of magnetic information between two magnetic layers.<sup>16</sup> As a particular example, it has been demonstrated<sup>17</sup> that spin-dependent transport properties of magnetic tunneling junctions strongly depend on the magnetic quantum well states existing therein. Moreover, the exchange interaction between ferromagnetic layers through a nonmagnetic medium can also be altered by quantum size effect.<sup>18-21</sup>

Electrons forming the QWS are usually of *s, p* character. Surprisingly, despite the localized nature of the *d* electrons,

the existence of *d* QWS has also been observed.<sup>22,23</sup> In addition, thickness-dependent electron reflectivity, for both spin channels, from Co thin films on Mo(110) has been measured.<sup>24</sup> In Refs. 8, 25, and 26 the authors report on the thickness dependence of the uniaxial magnetic anisotropy of supported Fe and Co multilayers, having a period of few monolayers. These variations were attributed to the presence of *d* QWS in the magnetic thin films. The interplay between quantum size effects and the MAE of nanosized systems has also been predicted by electronic-structure modeling.<sup>27-31</sup> In addition to the quantum size effect on MAE, alloying of supported Fe and Co adsorbates with large spin-orbit coupling elements often leads to an enhancement of MAE.<sup>32-34</sup>

The above-mentioned examples essentially take into account only two parameters, the chemical composition and the size of the nanostructures, in order to modify the magnetic properties. Alternatively, one can manipulate the electronic and magnetic properties of the nanostructures by using external electric field which affect the charge carriers of the nanosized systems.<sup>35-42</sup> For tuning the spin degrees of freedom of such systems, the electric field is preferred over the magnetic one due to its ability to control the magnetic properties in a local way.<sup>35,43</sup> It has been reported that the MAE in Fe monolayers<sup>32</sup> and quasi-1D systems<sup>33</sup> deposited on metal surfaces is highly sensitive to external electric field. In such systems, the variation of the magnetic properties is commonly attributed to the screening of the electric field at the surface. Since electric field screening involves redistribution of the surface charge, it should obviously affect the boundary conditions of the QWS, if the latter exist in the system.

In this paper, we investigate the interplay of the three factors described above (spin-polarized QWS, alloying and electric field) in Fe(Co) thin films on Pt(001) with their magnetic properties. We find that QWS in Fe(Co) thin films are predominantly of *d* character and have strong effect on the MAE. Tailoring the QWS by changing the film thickness, capping or applying external electric field provides the possibility to control MAE of thin metallic films. The physics of the underlying phenomena is discussed in terms of the second-order perturbation theory and Bruno relation.<sup>44,45</sup>

The rest of the paper is organized as follows: In Sec. II, the employed computational methods are briefly described. The results concerning the thickness dependence of the magnetic properties in the Fe(Co) thin films are presented in Sec. III, then the relationship between QWS and external electric field is discussed in Sec. IV. Finally, brief conclusions and perspectives are provided.

## II. COMPUTATIONAL METHODS

The calculations were performed within the density functional formalism as implemented in the *Vienna ab initio simulation package* (VASP) code<sup>46,47</sup> which is based on the supercell approach and employs projector augmented wave method (PAW) and a plane-wave basis set<sup>48</sup> for describing the Kohn-Sham wave functions. The local spin density approximation (LSDA) was used to describe the exchange-correlation interactions.<sup>49</sup> First, scalar relativistic calculations were carried out for the structural optimization of the systems. The force on each atom was minimized to be less than 5 meV/Å. It was found that the relaxations can not be neglected in the determination of the MAE. For instance, considering the bulk Pt-interlayer distance, 1.95 Å, as a reference, geometrical optimization reduces the interlayer distance between Fe(Co) and the outermost Pt layer of the substrate by  $\sim 28\%$ . As a second step, in order to calculate the MAE, defined as the energy difference between two directions of magnetization ( $E_x - E_z$ ) (see the inset in Fig. 1), fully relativistic self-consistent calculations including spin-orbit coupling were carried out. Since the MAE for these layered systems is expected to be relatively small ( $\sim$ few meV), a dense  $k$ -point mesh ( $19 \times 19 \times 1$ ) and large plane-wave energy cutoffs (400 eV) were employed in order to obtain an accurate MAE value. Denser  $k$ -point meshes and larger cutoff energies were tested for checking the reliability of the chosen parameters, resulting in insignificant changes of the results. Therefore, the parameters considered in this study are a good compromise between accuracy and computational effort.

The Fe(Co)-Pt multilayers are modeled by considering up to 9 ( $1 \leq N \leq 9$ ) layers of Co(Fe) and 10 Pt layers as the substrate. This choice assures that the surface electronic

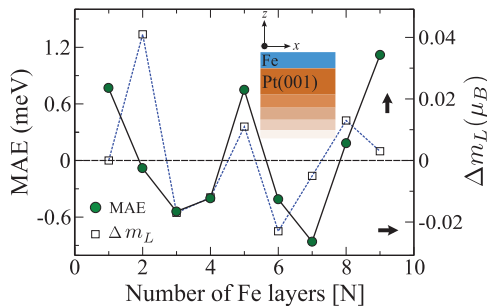


FIG. 1. (Color online) Magnetic anisotropy energy (circles) in meV, for  $\text{Fe}_N/\text{Pt}(001)$  multilayers as a function of the Fe thickness for  $1 \leq N \leq 9$ ,  $N$  being the number of Fe layers, is shown. A positive (negative) sign in MAE indicates an out-of-plane (in-plane) axis of magnetization (easy axis), respectively. Thickness dependence of the orbital moment anisotropy (OMA) of the multilayers (rectangles) in  $\mu_B$  is also presented.

structure in the layered systems is properly described. We have used 11 Å of vacuum space in the supercell in order to avoid possible interactions between periodic images.<sup>50</sup> When an external electric field was applied, the dipole corrections were also taken into account.<sup>51</sup> Hereafter, we shall denote our systems by the thickness of the magnetic multilayer as  $\text{Fe}(\text{Co})_N/\text{Pt}(001)$  or  $\text{Fe}(\text{Co})_N$ .

## III. MAGNETIC PROPERTIES OF Fe THIN FILMS ON Pt(001)

### A. Fe layers on Pt(001) surface

In order to study the dependence of the magnetic properties with respect to the magnetic film thickness, we calculate the MAE for different number of Fe layers deposited on Pt(001). For the case of a single Fe monolayer on Pt(001), we have found a MAE of 0.8 meV and an out-of-plane easy axis of magnetization, as shown in Fig. 1 (circles). For thicker Fe layers ( $2 \leq N \leq 9$ ),  $\text{Fe}_N/\text{Pt}(001)$ , the MAE varies exhibiting an oscillatory behavior, having a period of roughly four monolayers, and a switching of easy axis of magnetization. A strong out-of-plane MAE is observed for  $\text{Fe}_{5(9)}$  multilayers. A similar oscillatory behavior of the MAE has been observed in Fe films supported on Au(001) (Ref. 52) and Ag substrates.<sup>8</sup>

In ferromagnetic thin films such as Co and Fe multilayers, MAE can be understood in terms of the variations of the orbital-moment components. In general, the highest orbital-moment component lies in the direction of the easy axis. The link between MAE and orbital-moment anisotropy (OMA) ( $\Delta m_L = m_z^L - m_x^L$ ) is known as the Bruno's relation,  $\text{MAE} = \xi/4 (m_z^L - m_x^L)$ , where  $\xi$  is the spin-orbit constant of the magnetic layer.<sup>44,45</sup> In Fig. 1, the value of the OMA, difference of the orbital moment between two directions of magnetization, as a function of Fe thickness is also plotted and compared with the MAE behavior. One can observe that in almost all cases OMA exhibits a similar oscillatory trend as the MAE. Furthermore, in most cases the changes in MAE and OMA can be related to the occurrence of spin-polarized quantum well states in the iron thin films. To study the changes in the spin-polarized quantum well states, in Fig. 2 we plot the density of states (DOS) close to the  $\Gamma$  point<sup>53</sup> for Fe layers,  $3 \leq N \leq 8$ , in  $\text{Fe}_N/\text{Pt}(001)$  system.

It is observed that the spin-up (majority carriers) DOS is less sensitive to thickness variations (see Fig. 2). In contrast, the variation in the minority DOS is much more pronounced as the magnetic film thickness increases. The peaks of the minority DOS show a systematic shift with the thickness of the Fe layer which is a typical signature of the QWS existence. The peaks are mostly composed of  $d_{xz}$ ,  $d_{yz}$ , and  $d_{x^2-y^2}$  states, as shown in Fig. 2, then we can conclude that Fe films on Pt(001) support  $d$  QWS. The dashed lines represent the contribution of  $d_{xz}$  and  $d_{yz}$  orbitals, whereas dotted-dashed lines are the contribution of  $d_{x^2-y^2}$  orbitals. In addition, from the analysis on the orbital-resolved DOS we also observe  $s, p$  QWS, which have highly dispersive bands (have small effective masses), thus we believe that the variation of  $d_{x^2-y^2}$  orbitals is caused by  $s, p$  QWS via  $sp-d$  hybridization. It should be noted that the rest of the orbitals that are not presented in Fig. 2 have not shown a significant size-dependent effect. The variations

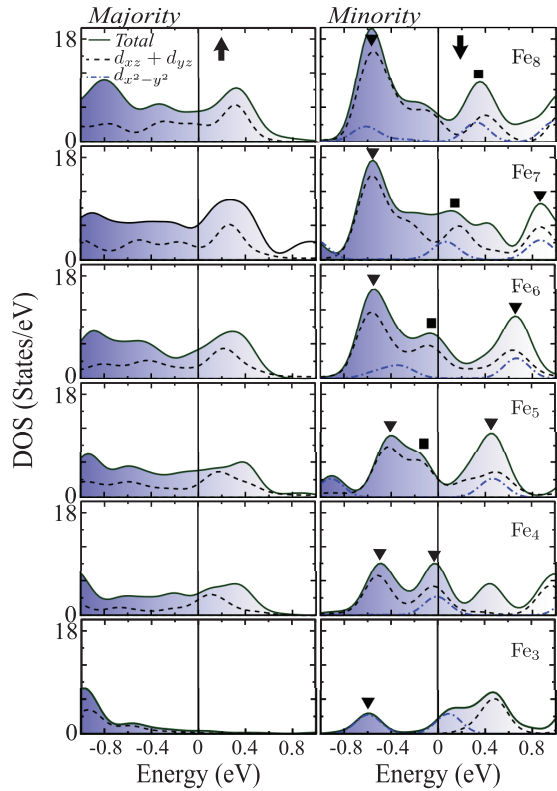


FIG. 2. (Color online) Majority (minority) density of states (DOS) (solid lines) for  $\text{Fe}_N/\text{Pt}(001)$  with  $3 \leq N \leq 8$ , close to the  $\Gamma$  is plotted. The dotted lines represent the contribution from both the  $d_{xz}$  and  $d_{yz}$  orbitals and the projection on  $d_{x^2-y^2}$  orbital is assigned by the dotted-dashed line. The triangle and rectangle arrows guide the shift in DOS as the Fe-film thickness is increased.

of the DOS can be directly associated with changes in MAE through the second-order perturbation formula<sup>44,45</sup>

$$\text{MAE} \propto \sum_{kl} \frac{|\langle u_k | \vec{l}_z | o_l \rangle|^2 - |\langle u_k | \vec{l}_x | o_l \rangle|^2}{\varepsilon_k - \varepsilon_l}, \quad (1)$$

where  $\vec{l}_x$  and  $\vec{l}_z$  are the angular momentum operators which couple the occupied ( $o_l$ ) and unoccupied ( $u_k$ ) states and  $\varepsilon_k(\varepsilon_l)$  are their respective eigenenergies. Clearly, the states close to the Fermi level are the ones which give the main contribution to the MAE. The analysis of the  $d$ -orbital matrix elements in Eq. (1) shows that the main contributions to MAE are determined by the coupling between the occupied and unoccupied states of  $d_{xy}$  with  $d_{x^2-y^2}$ , through  $\vec{l}_z$  operator, whereas the coupling of  $d_{xz(yz)}$  with  $d_{z^2}$  and  $d_{x^2-y^2}$  orbitals contribute negatively to the second part of Eq. (1). In Table I, the nature of the spin-orbit coupling matrix elements and the preferred direction of magnetization are provided.

From Fig. 2, one can see that the QWS lie close to Fermi energy in Fe films of four and seven layers. Whereas for five and eight layers of Fe, a depletion in the unoccupied  $d_{xz}$  and  $d_{yz}$  states above the Fermi level and smaller density of  $d_{x^2-y^2}$  orbitals close to the Fermi energy is observed. Hence, it will lead to a decrease in the coupling of  $\langle d_{xz(yz)} | l_x | d_{x^2-y^2} \rangle$ , which favors an in-plane magnetization (see Table I). Such strong reduction of the second term in Eq. (1) for the case of five and

TABLE I. The couplings between occupied and unoccupied states of different orbital symmetries and their contribution to the respective axis of magnetization. The vertical and horizontal arrows are assigned for in-plane and out-of-plane direction of magnetization, respectively.

$\langle o_k    u_l \rangle$	$d_{z^2}$	$d_{x^2-y^2}$
$d_{xy}$	$\sim 0$	$\uparrow$
$d_{xz}$	$\rightarrow$	$\rightarrow$
$d_{yz}$	$\rightarrow$	$\rightarrow$

eight Fe monolayers leads to an easy axis of magnetization perpendicular to the surface (shown in Fig. 2). On the contrary, for  $\text{Fe}_{4(7)}$ , the DOS close to the Fermi energy mainly consists of  $d_{xz(yz)}$  and  $d_{x^2-y^2}$  states, which also strongly favor an in-plane magnetization axis, via the coupling  $\langle d_{xz(yz)} | l_x | d_{x^2-y^2} \rangle$ , according to Eq. (1).

### B. Capping $\text{Fe}_N/\text{Pt}(001)$ with a Pt monolayer

We now investigate the effect of capping Fe multilayers with a single Pt layer. In these systems, the phase shift of the QWS at the vacuum side is altered as a result of the change in the boundary conditions. One thus could expect variations in the MAE as well. For thinner films, this variation could arise from the interface effect, but, for thicker films the change in the QWS could be dominant. It has been predicted that capping the Fe monolayer with nonmagnetic ones usually results in a strong enhancement of the MAE.<sup>32,54</sup> X-ray magnetic circular dichroism (XMCD) measurements at low temperature report a perpendicular magnetization for Pt-capped Fe monolayers (Fe-Pt alloy) on Pt.<sup>55</sup> In agreement with the previous results,<sup>32,55</sup> we also find a large MAE for Pt/Fe/Pt(001). For this particular system, MAE reaches  $\sim 5$  meV having an out-of-plane axis of magnetization. Such strong enhancement in MAE, in comparison with the uncapped Fe monolayer on Pt (0.8 meV), is attributed to a depletion in the minority  $d_{xz}$  and  $d_{yz}$  Fe orbitals near the Fermi energy, as a consequence of a strong hybridization of Fe with the capping Pt layer.<sup>54</sup>

For larger Fe thickness, namely,  $2 \leq N \leq 9$ , the magnetic properties in the Pt/Fe $_N$ /Pt(001) multilayers show strong thickness dependence, as can be seen in Fig. 3. For instance,

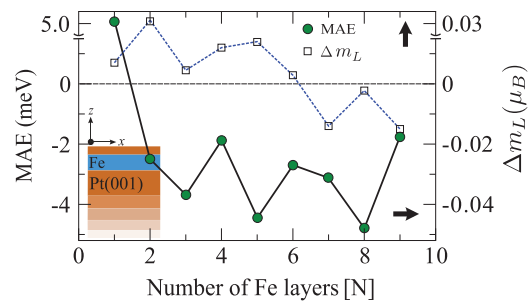


FIG. 3. (Color online) Magnetic anisotropy energy (MAE) in meV for Pt/Fe $_N$ /Pt(001) multilayers as a function of the Fe thickness,  $1 \leq N \leq 9$ , where  $N$  is the number of Fe layers plotted. A positive (negative) sign in MAE stands for a positive (negative) magnetization axis, respectively. The orbital magnetic moment difference versus the thickness of the film is also shown.

when a second Fe layer is added to the system, MAE abruptly decreases from  $\sim 5$  to  $\sim 2.5$  meV exhibiting magnetization reversal from out of plane to in plane at the same time. In this particular case, the Fe layers are partially hybridized with each other, the depleted  $d_{xz}$  and  $d_{yz}$  orbitals (for one Fe layer) close to the Fermi energy are restored, favoring an in-plane easy axis (see Table I). For  $N \geq 4$ , the MAE shows an oscillatory behavior and has roughly a value of 1.5 meV on average and the in-plane axis of magnetization remains.

In  $\text{Pt}/\text{Fe}_N/\text{Pt}(001)$ , the MAE variations can be analyzed in terms of the spin-polarized QWS, similar to the case of uncapped Fe multilayers. Furthermore, we have also presented the behavior of the orbital moments for the magnetic thin films. Interestingly, Bruno's relation is not fulfilled for this system. However, this could be explained by using a more generalized second-order perturbation treatment of the spin-orbit coupling, which also takes into account all the atomic species (magnetic and nonmagnetic).<sup>45,56</sup> Since the Pt atoms have a large spin-orbit coupling, they strongly hybridize with the Fe layers, hence, the spin-flip contribution term ( $\Delta E^{\uparrow\downarrow}$ ) is not negligible.<sup>45,56</sup>

It is also interesting to investigate how the spin polarization of the QWS near the Fermi level depends on the Fe thickness, for both capped and uncapped thin films, since the magnetic properties of the multilayers are mainly determined by the electrons near the Fermi energy. The spin polarization (SP) of the confined states in iron thin films can be defined as follows:  $\text{SP}(E) = [n_{\downarrow}(E) - n_{\uparrow}(E)]/[n_{\downarrow}(E) + n_{\uparrow}(E)]$ , where  $n_{\downarrow(\uparrow)}(E)$  stands for the minority (majority) DOS, respectively. In Fig. 4, the spin polarization of the QWS averaged from the values of SP close to the Fermi energy [ $\text{SP}(E_f)$  and  $\text{SP}(E_f \pm 0.1$  eV)] is presented as a function of the Fe thickness for both capped (circles) and uncapped (rectangles) Fe multilayers. First, it is observed that the SP is sensitive to the Fe thickness, for instance, in the case of uncapped Fe multilayers the SP for single Fe monolayer varies from having 45% (minority polarization) to 60% (majority polarization) after adding one more Fe layer [ $\text{Fe}_2/\text{Pt}(001)$ ], as can be seen in Fig. 4. Indeed, it is also shown that SP can be switched from positive to negative polarization depending on the thickness of Fe thin film. Additionally, an oscillating SP behavior was also observed (Fig. 4) as the number of Fe layers is increased. Thicker

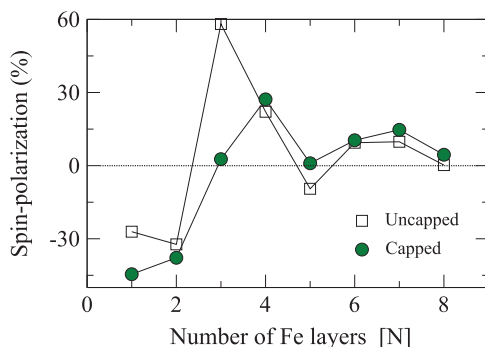


FIG. 4. (Color online) The average spin polarization of QWS, close to the  $E_f$  in  $\text{Fe}_N/\text{Pt}(001)$  (rectangles) and  $\text{Pt}/\text{Fe}_N/\text{Pt}(001)$  (circles) as a function of Fe thickness is drawn. The SP is averaged from the value of SP at  $E_f + 0.1$  eV,  $E_f$  and  $E_f - 0.1$  eV.

Fe films ( $N \geq 5$ ) show a reduced SP having an asymptotic behavior. The variation of the SP as a function of thickness is a clear evidence for the existence of spin-dependent QWS. Nevertheless, it is found that capping the most of Fe multilayers with Pt monolayer has not a substantial effect on the SP, i.e., a similar trend in the behavior of SP is observed in both capped and uncapped Fe layers (see Fig. 4).

As a summary, the spin polarization of the Fe films on  $\text{Pt}(001)$  is rather sensitive to film thickness, which could be of use for designing spintronic applications based, e.g., on spin-density waves. Experimentally, the SP of Fe and Co thin films could be investigated with scanning tunneling spectroscopy<sup>57</sup> (STS) since the DOS profile for the top two layers of Fe is similar to the DOS presented in our study. Our investigations on QWS and SP also suggest that the spin-dependent transport in similar systems could also be influenced by the quantum size effect phenomena.<sup>57,58</sup>

#### IV. MAGNETIC PROPERTIES OF Co THIN FILMS ON $\text{Pt}(001)$

To explore the role of the chemical composition on magnetic thin films, we have investigated Co multilayers, in the same way as in the case of Fe multilayers (Sec. III). First, the results concerning Co multilayers on  $\text{Pt}(001)$  are discussed. We show that Co thin films can also host  $d$  QWS. The MAE as a function of the Co thickness is presented in Fig. 5(a). Our theoretical study predicts values of MAE for a single and two Co layers on  $\text{Pt}(001)$ , to be 0.4 and 1.2 meV, respectively, having an in-plane direction of magnetization. Larger Co thickness also shows an in-plane axis of magnetization, except for the case of  $\text{Co}_5/\text{Pt}(001)$ , which has an out-of-plane axis of magnetization ( $\sim 0.1$  meV). These results are in agreement with experimental results for Co films on  $\text{Pt}(001)$  and  $\text{Pd}(001)$

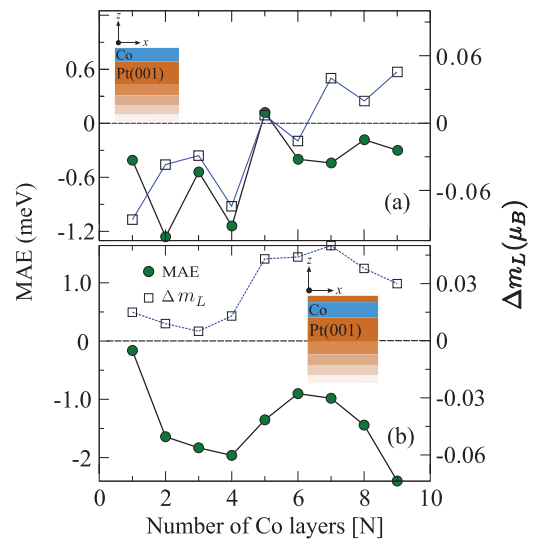


FIG. 5. (Color online) Magnetic anisotropy energy (circles) of (a)  $\text{Co}_N/\text{Pt}(001)$  and (b)  $\text{Pt}/\text{Co}_N/\text{Pt}(001)$  multilayers as a function of the Co thickness for  $1 \leq N \leq 9$  is shown, where  $N$  is assigned for the number of Co layers. A positive (negative) sign in MAE indicates an out-of plane (in-plane) easy axis, respectively. Thickness dependence of the orbital moment anisotropy (OMA) of the multilayers (rectangles) in  $\mu_B$  is also presented.



having thickness  $\geq 5 \text{ \AA}$  which report an in-plane easy axis.<sup>59,60</sup> The OMA as a function of the Co thickness is also calculated and shown in Fig. 5(a). For six layers of Co or less, the MAE and OMA are proportional to each other, according to the Bruno's relation. For these cases, we can explain the correlation between the MAE and the spin-polarized QWS of the Co thin films, in an analogous way to the case of  $\text{Fe}_N/\text{Pt}(001)$ .

The results concerning the magnetic properties of Pt-capped Co films are now presented. In Fig. 5(b), the MAE and orbital anisotropy show an oscillatory behavior with respect to the number of Co layers, and the periods of oscillation of the MAE is estimated to be 5 monolayers. This period of oscillation is comparable with other theoretical study of Co multilayers supported by Pd.<sup>28</sup> It is also shown that capping Co multilayers with Pt increases the value of the MAE for all layers, except for the case of the Co monolayer. The easy axis of magnetization for all Co multilayers points in plane. These results are in agreement with experimental measurements which show in-plane easy axis for a Pt-capped Co multilayer.<sup>59</sup> In addition, the orbital-moment differences ( $\Delta m_L = m_z^L - m_x^L$ ) of  $\text{Pt}/\text{Co}_N/\text{Pt}(001)$  system are presented in Fig. 5(b). The interesting finding is that the profile for MAE and OMA is symmetrically inverted with respect to each other, i.e., the highest value of the orbital moment is always perpendicular to the surface (parallel to the  $z$  axis). Such incompatibility of OMA with MAE is explained in Sec. III B, by arguing that the spin-flip contribution ( $\Delta E^{\uparrow\downarrow}$ ) is non-negligible.<sup>45,56</sup>

In Fig. 6, the majority and minority DOS for Co multilayers ( $3 \leq N \leq 8$ ) on  $\text{Pt}(001)$  and the  $d$  orbitals which give the highest contribution to DOS, namely,  $d_{xz(yz)}$ ,  $d_{x^2-y^2}$ , and  $d_{z^2}$ , are plotted. As in the case of Fe multilayers, the majority DOS shows insignificant variation, and the QWS of the minority carriers are driven by  $d_{xz(yz)}$  (dashed lines) and  $d_{x^2-y^2}$  (dotted lines) orbitals. However, for  $N \leq 4$  the minority  $d_{z^2}$  (dashed-dotted lines) component also contributes to the QWS moving towards the Fermi energy from the unoccupied states. Here, we have pointed out that the magnetic layers undergo strong changes in the DOS (Fig. 6, dashed lines) if the thickness of the film is modified. The projection of majority  $d_{z^2}$  is negligibly small and has been omitted.

To understand the thickness dependence of the MAE, we have analyzed the spin-orbit matrix elements, and it was found that the coupling between occupied and unoccupied states of  $d_{xz}$  ( $d_{yz}$ ) with  $d_{z^2}$  and  $d_{x^2-y^2}$  orbitals are dominant compared to the other couplings (see Table I), hence favoring an in-plane axis of magnetization [second term in Eq. (1)], which is the case for most Co-layer thicknesses. The correspondence between the changes in the DOS (Fig. 6) and MAE (on Fig. 5) is then analyzed. For example, from Fig. 6 the QWS of  $d_{xz(yz)}$  and  $d_{x^2-y^2}$  orbitals cross the Fermi energy at six layers of Co. Thus, as a result of the coupling ( $\langle d_{xy} | l_z | d_{x^2-y^2} \rangle$ ) the magnitude of the in-plane MAE is reduced, which is the first matrix element of Eq. (1). As a conclusion, both occupied and unoccupied QWS are mainly of  $d_{xz(yz)}$ ,  $d_{x^2-y^2}$ , and  $d_{z^2}$  characters, and the distribution of these orbitals near the Fermi energy establishes the connection between the enhanced (reduced) in-plane MAE and the QWS.

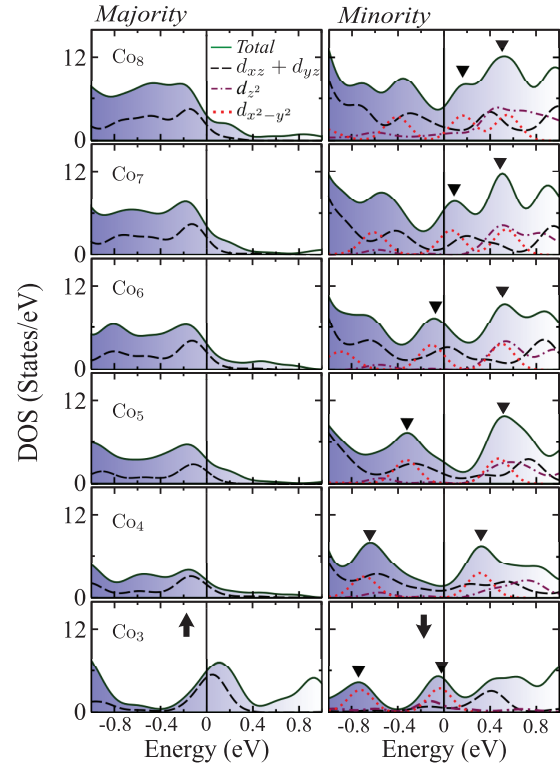


FIG. 6. (Color online) Majority and minority DOS of Pt-capped Co multilayer on  $\text{Pt}(001)$ , close to the  $\Gamma$  point, are plotted. The DOS are plotted for Co multilayers in the range  $3 \leq N \leq 8$ . The dashed, dashed-dotted, and dotted lines represent the contribution from  $d_{xz(yz)}$ ,  $d_{z^2}$ , and  $d_{x^2-y^2}$  orbitals, respectively. The triangle arrows guide the shift in the DOS.

Regarding the spin polarization near the Fermi energy for Co multilayers, in Fig. 7 we plot the average SP of the QWS with respect to the film thickness. For both capped and uncapped Co multilayers, the SP strongly varies when the thickness changes. For instance, the SP for three and four layers of Co can be as large as  $+60\%$  and  $-5\%$ , respectively. In almost all Co multilayers, the SP is positive with an exception of four monolayers of Co ( $\text{Co}_4$ ). Different from the results of Fe multilayers, here, capping thin films of Co with Pt strongly

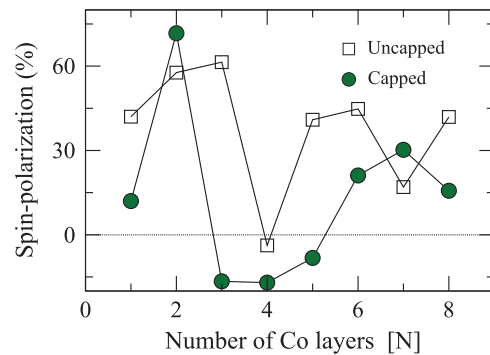


FIG. 7. (Color online) The average spin polarization of QWS, close to the Fermi energy, in  $\text{Co}_N/\text{Pt}(001)$  (rectangles) and  $\text{Pt}/\text{Co}_N/\text{Pt}(001)$  (circles) as a function of Co thickness is drawn. The SP is averaged from the value of SP at  $E_f + 0.1 \text{ eV}$ ,  $E_f$  and  $E_f - 0.1 \text{ eV}$ .

affects the SP. As an illustration, capping of three and five ( $\text{Co}_{3(5)}$ ) layers of Co with Pt induces a switch in the spin polarization. From Fig. 7 one can see that thicker films of Co ( $N \geq 5$ ) have higher tendency to be polarized, as compared to Fe thin films. Further, from the respective plots of SP for Fe and Co, it is observed that the first few Co thin films ( $N \leq 2$ ) are oppositely polarized in contrast to the Fe thin films.

### V. EFFECT OF ELECTRIC FIELD ON QWS AND MAGNETIC PROPERTIES

Once we have investigated the interplay of size and chemical composition of Fe(Co) multilayers on Pt with QWS, MAE, and SP, we draw our attention to the possibility of controlling QWS (and hence the MAE) with external electric field. In order to demonstrate this phenomena, we have chosen Pt-capped Fe multilayers as a sample system. Basically, when an electric field is introduced, the electrostatic potential near the capping layer is strongly modified and causes a charge redistribution at the interface. As explained in Sec. II, the Pt atoms which have high spin-orbit coupling hybridize well with the magnetic atoms, and this determines the magnetic features of the film. Hence, for Fe layers in Pt/ $\text{Fe}_N$ /Pt(001) structure the external electric field affects the hybridization of Fe(Co) and Pt, and such variation on the Fe(Co)-Pt interface will change the magnetic properties of the film. In order to quantify this effect, an electric field is applied for all thicknesses of Fe in the capped system.

The response of the MAE to the external electric field, which follows nearly linear behavior, is presented in Fig. 8(a) for the case of four layers of Fe in Pt/ $\text{Fe}_N$ /Pt(001) system. Meanwhile, in order to investigate how sensitive the MAE

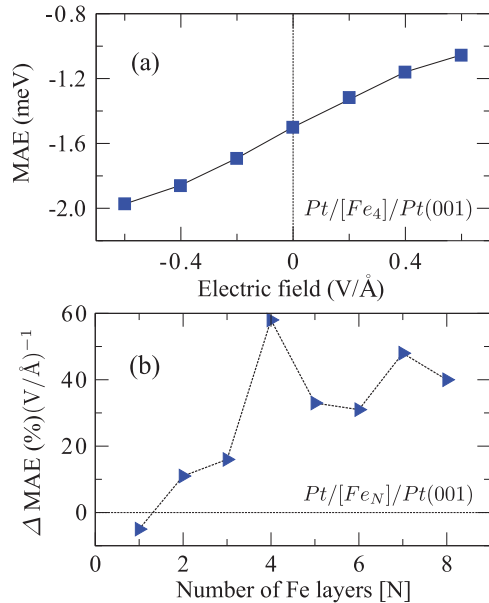


FIG. 8. (Color online) (a) The MAE as function of external electric field for Pt/ $\text{Fe}_4$ /Pt(001) supercell. (b) The rate of change of the MAE ( $\Delta\text{MAE}$ ), in percents per  $\text{V}/\text{\AA}$ , as a result of an external electric field normalized by the MAE of the neutral system, for a different number of Fe layers of Pt/ $\text{Fe}_N$ /Pt(001) system. The  $\Delta\text{MAE}$  is evaluated for  $E_+ = 0.4$  and  $E_- = -0.4$  [see Eq. (2)].

of metallic thin films reacts to an external electric field, in Fig. 8(b) the rate of change of the magnetic anisotropy energy ( $\Delta\text{MAE}$ ) with respect to electric field is presented for all thicknesses of Fe in Pt/ $\text{Fe}_N$ /Pt(001). We quantify this rate as follows:

$$\Delta\text{MAE} = \left[ \frac{\text{MAE}(E_-) - \text{MAE}(E_+)}{|E_- - E_+| \text{MAE}(0)} \right] \times 100\%, \quad (2)$$

where  $[\text{MAE}(E_-)]\text{MAE}(E_+)$  is the magnetic anisotropy energies at (negative) positive electric field, whereas  $\text{MAE}(0)$  is the value of MAE for the neutral system [see Eq. (2)]. The rate of change of the MAE ( $\Delta\text{MAE}$ ) (in percents per  $\text{V}/\text{\AA}$  for  $E_+ = 0.4$  and  $E_- = -0.4$ ) is shown in Fig. 8(b). As an illustration, the  $\Delta\text{MAE}$  of four layers of Fe is found to be  $\sim 60\%$  per  $\text{V}/\text{\AA}$ . Our calculations reveal that for all Fe layers, except for one layer of Fe, a negative electric field increases the MAE, i.e., only in the case of single Fe layer the response is opposite with respect to the larger thicknesses. For all other multilayers ( $2 \leq N \leq 8$ ), the rate of change of MAE is positive in sign, showing an oscillatory behavior as the thickness of Fe layers is increased.

Generally, when a negative electric field is applied it has a tendency to favor an in-plane magnetization, i.e., negative electric field decreases out-of plane MAE ( $N = 1$ ) and increases the absolute value of in-plane MAE ( $2 \leq N \leq 8$ ), compared to the neutral system. Moreover, as can be seen in Fig. 8(b),  $\Delta\text{MAE}$  has the highest value of  $\sim 60\%$  for  $N = 4$ , and oscillates as the number of Fe layers increase. The peaks in the  $\Delta\text{MAE}$  for thicker thin films [e.g. Pt/ $\text{Fe}_{4(7)}$ /Pt(001)] can be associated with the influence of the external electric field on QWS other than the contribution only from Fe-Pt interface. On the other hand, the SP of the QWS is also affected by the electric field, for instance, five and six Fe layers exhibit an increase in the SP around the Fermi energy by 14% and 11%, respectively, upon exposure to an electric field of 1  $\text{V}/\text{\AA}$ .

In relation to the above discussion, i.e., variations of the MAE and SP by electric field, as an example, the Kohn-Sham levels close to the  $\Gamma$  point for four layers of Fe are plotted in Fig. 9. The Kohn-Sham levels (close to the Fermi energy) which have nonzero occupation (occupations  $\geq 0.04$ ) by the orbitals, namely,  $s + p$ ,  $d_{xz(yz)}$ , and  $d_{x^2-y^2}$ , are presented. The eigenenergies are plotted for external electric field of  $-0.4$  and  $0.4 \text{ V}/\text{\AA}$ . Both majority and minority states are shifted as result of external electric field which resembles a Stark shift. Moreover, one can see that the shift of the  $d_{xz(yz)}$  and  $d_{x^2-y^2}$  band energies is correlated to  $s + p$  ones, and thus it is an evidence that the effect of electric field on  $d$  states is mediated by  $s + p$  states via the mixed orbitals.

A robust correlation between rate of change of MAE and the DOS has occurred. In Sec. II, our analysis showed that there exists an overlap between  $sp$  and  $d$  orbitals, specifically,  $d_{xz(yz)}$  and  $d_{x^2-y^2}$  orbitals. Hence, the response to the electric field mainly involves the  $sp$  QWS and modifies the  $d$  states by  $sp-d$  hybridization. Specifically, the peaks in the  $\Delta\text{MAE}$  for Pt/ $\text{Fe}_{4(7)}$ /Pt(001) systems are caused by the high density of  $d_{xz(yz)}$  and  $d_{x^2-y^2}$  orbitals, as analyzed in the orbital-resolved DOS. Both orbitals are affected by  $sp$  QWS, but the former orbitals are higher in density (close to  $E_f$ ). This implies that when the  $d_{xz(yz)}$  and  $d_{x^2-y^2}$  orbitals are highly degenerated

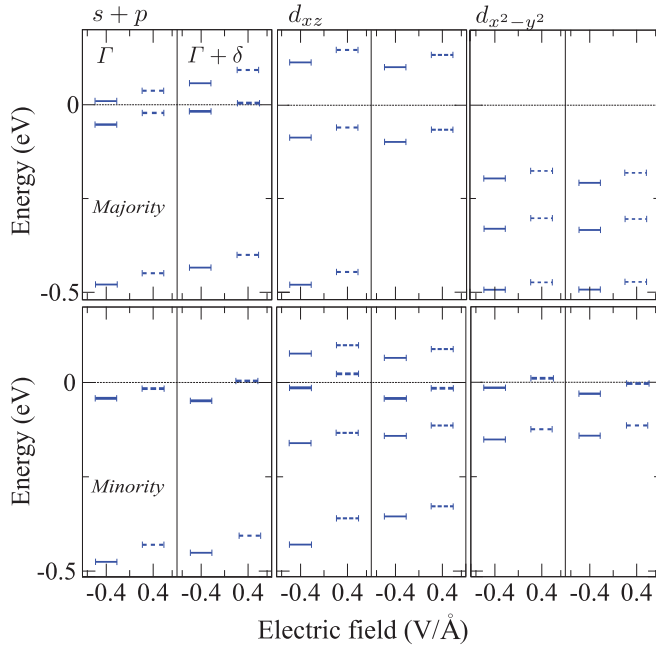


FIG. 9. (Color online) The Kohn-Sham eigenenergies close to the  $\Gamma$  point for which the  $s + p$ ,  $d_{xz}$ , and  $d_{x^2-y^2}$  orbitals of four layers of Fe [Pt/Fe<sub>4</sub>/Pt(001)] have high contribution. The energy of the electronic levels (relative to the Fermi energy) is presented for an electric field of  $0.4 \text{ V/\AA}$  (dashed lines) and  $-0.4 \text{ V/\AA}$  (full lines), and two  $k$  points,  $\Gamma$  and  $\Gamma + \delta$  points, have been considered ( $\delta = 0.03 \text{ \AA}^{-1}$ ).

close to the Fermi energy, the response to the external electric field is enhanced.

The variations of the MAE and SP can be explicitly associated with the shift of the Kohn-Sham energy levels. The analysis on the orbital-resolved DOS reveals that the minority bands of Fe multilayers near the Fermi energy are dominated by  $d_{xz(yz)}$  and  $d_{x^2-y^2}$  states. Hence, for negative electric field, we observe the shift of the Kohn-Sham eigenenergies

towards lower energy levels, and even a crossing of the Fermi energy (Fig. 9). Furthermore, as a result of negative electric field, the increase in the DOS of unoccupied  $d_{xz(yz)}$  and  $d_{x^2-y^2}$  orbitals near the Fermi energy affects the coupling of  $\langle d_{xz(yz)} | l_x | d_{x^2-y^2} \rangle$ , where this coupling favors an in-plane axis of magnetization (Table I). Recalling the second-order perturbation theory, the higher number of bands for  $d_{xz(yz)}$  and  $d_{x^2-y^2}$  orbital near the Fermi energy is accountable for the increase in the absolute value of the MAE, when a negative electric field is applied. It increases the contribution to the second term of Eq. (1) and has a net effect of favoring an in-plane magnetization.

The investigations of the effect of electric field on the MAE of Co thin films have been carried out. The results show that the MAE of Pt/Co<sub>N</sub>/Pt(001) linearly varies with respect to the electric field strength. Furthermore, the rate of change of MAE ( $\Delta\text{MAE}$ ) [Eq. (2)] oscillates as the Co thickness is increased. As an example, it was found that the MAE can be tuned up to 56% in the presence of an electric field of  $1 \text{ V/\AA}$ , as compared to the neutral system.

## VI. CONCLUSION

Our investigations demonstrated the possibility of controlling the MAE of Fe(Co) thin films by changing the film thickness and external electric field. These variations are mediated by the spin-dependent quantum well states. For almost all magnetic thin films, capping strongly enhances the MAE. The changes in the magnetic anisotropy energy can be explained by using the second-order perturbation theory. Additionally, a transition of the SP of the QWS was observed as the size of the thin film increases. The MAE and SP are sensitive to the external electric field, and substantial change of MAE can be achieved therewith. We believe that the results presented in this work can be additional ingredients for the understanding and engineering of spintronic and magnetoelectric devices.

<sup>1</sup>J. E. Ortega and F. J. Himpsel, *Phys. Rev. Lett.* **69**, 844 (1992).

<sup>2</sup>J. P. Sun, G. I. Haddad, P. Mazumder, and J. N. Schulman, *Proc. IEEE* **86**, 641 (1998).

<sup>3</sup>V. B. Sandomirskii, *Sov. Phys.-JETP* **25**, 101 (1967) [*JETP* **52**, 158 (1967)].

<sup>4</sup>A. L. Vázquez de Parga, J. J. Hinarejos, F. Calleja, J. Camarero, R. Otero, and R. Miranda, *Surf. Sci.* **603**, 1389 (2009).

<sup>5</sup>W. B. Su, C. S. Chang, and T. T. Tsong, *J. Phys. D: Appl. Phys.* **43**, 013001 (2010).

<sup>6</sup>Y. Guo, Y.-F. Zhang, X.-Y. Bao, T.-Z. Han, Z. Tang, L.-X. Zhang, W.-G. Zhu, E. G. Wang, Q. Niu, Z. Q. Qiu, J.-F. Jia, Z.-X. Zhao, and Q.-K. Xue, *Science* **306**, 1915 (2004).

<sup>7</sup>N. Binggeli and M. Altarelli, *Phys. Rev. Lett.* **96**, 036805 (2006).

<sup>8</sup>J. Li, M. Przybylski, F. Yildiz, X. D. Ma, and Y. Z. Wu, *Phys. Rev. Lett.* **102**, 207206 (2009).

<sup>9</sup>R. K. Kawakami, E. Rotenberg, H. J. Choi, E. J. Escorcia-Aparicio, M. O. Bowen, J. H. Wolfe, E. Arenholz, Z. D. Zhang, N. V. Smith, and Z. Q. Qiu, *Nature (London)* **398**, 132 (1999).

<sup>10</sup>F. J. Himpsel, *Phys. Rev. B* **44**, 5966 (1991).

<sup>11</sup>S. Zhang, *Phys. Rev. Lett.* **83**, 640 (1999).

<sup>12</sup>P. Gambardella, A. Dallmeyer, K. Maiti, M. C. Malagoli, S. Rusponi, P. Ohresser, W. Eberhardt, C. Carbone, and K. Kern, *Phys. Rev. Lett.* **93**, 077203 (2004).

<sup>13</sup>A. J. Freeman and R.-Q. Wu, *J. Magn. Magn. Mater.* **100**, 497 (1991).

<sup>14</sup>W. Weber, A. Bischof, R. Allenspach, C. Wursch, C. H. Back, and D. Pescia, *Phys. Rev. Lett.* **76**, 3424 (1996).

<sup>15</sup>C. Wursch, C. Stamm, S. Egger, D. Pescia, W. Baltensperger, and J. S. Helman, *Nature (London)* **389**, 937 (1997).

<sup>16</sup>K. N. Altmann, W. O'Brien, D. J. Seo, F. J. Himpsel, J. E. Ortega, A. Naermann, P. Segovia, A. Mascaraque, and E. G. Michel, *J. Electron. Spectrosc.* **101**, 367 (1999).

<sup>17</sup>Z.-Y. Lu, X.-G. Zhang, and S. T. Pantelides, *Phys. Rev. Lett.* **94**, 207210 (2005).

<sup>18</sup>P. Bruno and C. Chappert, *Phys. Rev. Lett.* **67**, 1602 (1991).

<sup>19</sup>P. Bruno and C. Chappert, *Phys. Rev. B* **46**, 261 (1992).

<sup>20</sup>O. O. Brovko, P. A. Ignatiev, V. S. Stepanyuk, and P. Bruno, *Phys. Rev. Lett.* **101**, 036809 (2008).

- <sup>21</sup>P. Lang, L. Nordstrom, R. Zeller, and P. H. Dederichs, *Phys. Rev. Lett.* **71**, 1927 (1993).
- <sup>22</sup>K. Yoshimatsu, K. Horiba, H. Kumigashira, T. Yoshida, A. Fujimori, and M. Oshima, *Science* **333**, 319 (2011).
- <sup>23</sup>D. A. Luh, J. J. Paggel, T. Miller, and T.-C. Chiang, *Phys. Rev. Lett.* **84**, 3410 (2000).
- <sup>24</sup>J. S. Park, A. Quesada, Y. Meng, J. Li, E. Jin, H. Son, A. Tan, J. Wu, C. Hwang, H. W. Zhao, A. K. Schmid, and Z. Q. Qiu, *Phys. Rev. B* **83**, 113405 (2011).
- <sup>25</sup>M. Przybylski, M. Dabrowski, U. Bauer, M. Cinal, and J. Kirschner, *J. Appl. Phys.* **111**, 07C102 (2012).
- <sup>26</sup>U. Bauer, M. Dabrowski, M. Przybylski, and J. Kirschner, *Phys. Rev. B* **84**, 144433 (2011).
- <sup>27</sup>P. van Gelderen, S. Crampin, and J. E. Inglesfield, *Phys. Rev. B* **53**, 9115 (1996).
- <sup>28</sup>M. Cinal and D. M. Edwards, *Phys. Rev. B* **57**, 100 (1998).
- <sup>29</sup>M. Cinal, *J. Phys.: Condens. Matter* **13**, 901 (2001).
- <sup>30</sup>L. Szunyogh, B. Ujfalussy, C. Blaas, U. Pustogowa, C. Sommers, and P. Weinberger, *Phys. Rev. B* **56**, 14036 (1997).
- <sup>31</sup>M. Cinal, *J. Phys.: Condens. Matter* **15**, 29 (2003).
- <sup>32</sup>M. Tsujikawa and T. Oda, *Phys. Rev. Lett.* **102**, 247203 (2009).
- <sup>33</sup>T. R. Dasa, P. A. Ignatiev, and V. S. Stepanyuk, *Phys. Rev. B* **85**, 205447 (2012).
- <sup>34</sup>G. Y. Guo, *J. Phys.: Condens. Matter* **11**, 4329 (1999).
- <sup>35</sup>E. Y. Tsybal, *Nature Mater.* **11**, 12 (2012).
- <sup>36</sup>K. Nakamura, R. Shimabukuro, T. Akiyama, T. Ito, and A. J. Freeman, *Phys. Rev. B* **80**, 172402 (2009).
- <sup>37</sup>P. Ruiz-Díaz, T. R. Dasa, and V. S. Stepanyuk, *Phys. Rev. Lett.* **110**, 267203 (2013).
- <sup>38</sup>N. N. Negulyaev, V. S. Stepanyuk, W. Hergert, and J. Kirschner, *Phys. Rev. Lett.* **106**, 037202 (2011).
- <sup>39</sup>K. Berland, T. L. Einstein, and P. Hylgaard, *Phys. Rev. B* **85**, 035427 (2012).
- <sup>40</sup>P. A. Ignatiev and V. S. Stepanyuk, *Phys. Rev. B* **84**, 075421 (2011).
- <sup>41</sup>N. Bonnet and N. Marzari, *Phys. Rev. Lett.* **110**, 086104 (2013).
- <sup>42</sup>J. Hu and R. Wu, *Phys. Rev. Lett.* **110**, 097202 (2013).
- <sup>43</sup>N. A. Spaldin and M. Feibig, *Science* **309**, 391 (2005).
- <sup>44</sup>D. S. Wang, R. Wu, and A. J. Freeman, *Phys. Rev. B* **47**, 14932 (1993).
- <sup>45</sup>P. Bruno, *Phys. Rev. B* **39**, 865 (1989).
- <sup>46</sup>G. Kresse and J. Hafner, *Phys. Rev. B* **47**, 558 (1993).
- <sup>47</sup>G. Kresse and J. Furthmüller, *Phys. Rev. B* **54**, 11169 (1996).
- <sup>48</sup>G. Kresse and D. Joubert, *Phys. Rev. B* **59**, 1758 (1999).
- <sup>49</sup>D. M. Ceperley and B. J. Alder, *Phys. Rev. Lett.* **45**, 566 (1980).
- <sup>50</sup>We have checked the convergence of the MAE with respect to the vacuum distance; for vacuum layer distance of 14 Å the MAE changes only by 3%. Thus, such variation of the MAE will not alter the conclusion presented in this paper.
- <sup>51</sup>J. Neugebauer and M. Scheffler, *Phys. Rev. B* **46**, 16067 (1992).
- <sup>52</sup>C. Liu and S. D. Bader, *J. Vac. Sci. Technol. A* **8**, 2727 (1990).
- <sup>53</sup>The states close to the  $\Gamma$  point are expected to have the highest contribution to the quantum well states (Refs. 7 and 28).
- <sup>54</sup>M. Tsujikawa, A. Hosokawa, and T. Oda, *Phys. Rev. B* **77**, 054413 (2008).
- <sup>55</sup>S. Imada, A. Yamasaki, S. Suga, T. Shima, and K. Takahashi, *Appl. Phys. Lett.* **90**, 132507 (2007).
- <sup>56</sup>C. Andersson, B. Sanyal, O. Eriksson, L. Nordström, O. Karis, D. Arvanitis, T. Konishi, E. Holub Krappe, and J. H. Dunn, *Phys. Rev. Lett.* **99**, 177207 (2007).
- <sup>57</sup>H. Oka, P. A. Ignatiev, S. Wedekind, G. Rodary, L. Niebergall, V. S. Stepanyuk, D. Sander, and J. Kirschner, *Science* **327**, 843 (2010).
- <sup>58</sup>H. Oka, K. Tao, S. Wedekind, G. Rodary, V. S. Stepanyuk, D. Sander, and J. Kirschner, *Phys. Rev. Lett.* **107**, 187201 (2011).
- <sup>59</sup>S. M. Valvidares, T. Schroeder, O. Robach, C. Quiros, T.-L. Lee, and S. Ferrer, *Phys. Rev. B* **70**, 224413 (2004).
- <sup>60</sup>H. L. Meyerheim, M. Przybylski, A. Ernst, Y. Shi, J. Henk, E. Soyka, and J. Kirschner, *Phys. Rev. B* **76**, 035425 (2007).